Numerical Solution and Stability Analysis of the Burgers Equation Based on SPH Method

Rui Zhao, Rahmatjan Imin

Abstract—**This paper employs Smoothed Particle Hydrodynamics (SPH) to solve the Burgers equation and proposes a semi-implicit scheme with unconditional stability. The accuracy and robustness of SPH and kernel Derivative Free-SPH (KDF-SPH) are demonstrated by several numerical tests, including the 1D, 2D, 3D Burgers equation in both regular irregular domains. Several test problems are presented to compare the results with other numerical methods in the literature. The findings reveal that KDF-SPH performs better in simulations, exhibiting lower errors. This study provides a new perspective on numerical simulations in fluid dynamics and offers a precise and efficient computational tool for researchers in related fields.**

Index Terms—**Burgers equation, Irregular domain, SPH, Stability analysis**

I. Introduction

Partial differential equations (PDEs) are fundamental mathematical tools for describing physical phenomena and engineering problems. They provide precise descriptions of how the state of a system changes over time and space, making them essential in fields such as theoretical physics, chemical dynamics, bioinformatics, and electrical engineering [1]. With the rapid advancement of science and technology, the applications of PDEs have expanded significantly, and their role in interdisciplinary research has grown increasingly important. Among these, reaction-diffusion equations are particularly noteworthy for their ability to model simultaneous diffusion and chemical reactions in a medium. PDEs also play a critical role in modeling wave propagation, heat transfer, fluid dynamics, and numerous other physical processes. Their capacity to capture complex interactions and behaviors makes them indispensable in both theoretical studies and practical applications. For instance, in bioinformatics, PDEs are widely used to model the spread of diseases and the dynamics of biological populations, while in electrical engineering, they describe electromagnetic wave propagation and signal processing.

Nonlinear PDEs are considerably more complicated than linear PDEs, and as a result, finding an exact solution is usually limited to simpler situations or certain types of equations. In such cases, numerical solutions may effectively solve these difficulties [2]. The complexity of nonlinear PDEs stems from their ability to model turbulence, shock waves, and chaotic behavior—phenomena that are inherently resistant to analytical treatment. This inherent complexity necessitates numerical approaches when analytical solutions prove intractable.

The Burgers equation exemplifies these characteristics by combining a linear diffusion term with nonlinearity. Proposed by J.M. Burgers in 1948 [3] to model fluid turbulence, it remains a crucial equation in the study of fluid mechanics and nonlinear dynamics. Recent computational advancements have broadened its applications to viscoelastic wave propagation, viscous shock waves, gas transport, semiconductor diffusion, and combustion processes [4]. Its nonlinearity can lead to the formation of shock waves in finite time, making the Burgers equation an excellent benchmark for testing numerical methods in fluid dynamics.

Numerous scholars have proposed various numerical solutions to the Burgers equation. For instance, Chen [5] employed finite difference methods and conducted an error analysis, while Wang et al. [6] developed a fourth-order implicit compact difference scheme that conserves energy. Zhang et al. [7] applied a linearized compact difference scheme to solve a two-dimensional Sobolev equation featuring a Burgers-type nonlinear term. Xu et al. [8] introduced modified non-conforming finite element schemes for nonlinear Burgers equations and performed a super-convergence analysis. Additionally, Wang et al. [9] developed a multi-region Galerkin approach, and Zhao et al. [10] utilized a space-time continuous Galerkin method to solve the 2D Burgers equation. Wang et al. [11] also employed a weak Galerkin finite element method to solve Burgers equations with fractional time derivatives. While these methods ensure numerical accuracy, they are heavily dependent on mesh discretization, which can affect the quality of results and incur substantial computational costs. Furthermore, these methods encounter challenges when dealing with irregular domains. Despite their accuracy, mesh-dependent methods face significant challenges in handling high-dimensional problems or irregular domains, where mesh generation becomes computationally prohibitive. Moreover, adaptive mesh refinement techniques often introduce additional complexity, limiting their practicality in dynamic simulations. These limitations motivate the exploration of mesh-free alternatives, such as SPH, which inherently bypass grid-related constraints. To overcome the limitations of mesh-dependent methods, mesh-free methods have been developed, which do not require grid generation. Prominent mesh-free methods include Smoothed Particle

Manuscript received January 27, 2025; revised April 18, 2025. This study was supported by the Natural Science Foundation of Xinjiang, China (Grant No. 2024D01C44).

Rui Zhao is a postgraduate of the College of Mathematical and Systems Science, Xinjiang University, Urumqi 830017, China (e-mail: 107552300623@stu.xju.edu.cn).

Rahmatjan Imin is an associate professor of the College of Mathematical and Systems Science, Xinjiang University, Urumqi 830017, China (corresponding author, e-mail: rahmatjanim@xju.edu.cn).

Hydrodynamics (SPH), Discrete Element Method (DEM), and Element-Free Galerkin Method (EFG) [12]–[17]. SPH, initially proposed by Lucy [18] and Gingold [19] in 1977, has found widespread application in astrophysical simulations. This method combines the advantages of being mesh-free, Lagrangian, and particle-based [20], [21], making it particularly suitable for simulating large deformations, free surface flows, and complex interface motions [22]–[25]. However, traditional SPH has faced criticism for its lower accuracy, prompting the development of enhanced versions such as Corrective Smoothed Particle Hydrodynamics (CSPH), Moving Least Squares Particle Hydrodynamics (MLSPH), and KDF-SPH.

In this paper, we aim to solve the Burgers equation using two SPH methods: conventional SPH and KDF-SPH. The time derivative are addressed using the Euler method, while SPH is employed to approximate the spatial derivatives, resulting in a semi-implicit discretization scheme. We analyze the stability of the scheme using the spectral radius criterion, demonstrating that both methods are unconditionally stable. To evaluate their reliability, accuracy, and efficiency, we conduct numerical simulations of the Burgers equation in 1D, 2D, and 3D cases, including irregular domains. The results confirm the stability, effectiveness, and high efficiency of the proposed schemes. Comparisons of errors indicate that KDF-SPH yields smaller errors and provides superior simulation results, making it more suitable for solving the Burgers equation.

The paper is organized as follows: Section 2 provides a detailed explanation of the tensor representation of the Burgers equation. Section 3 introduces the kernel approximations for the two SPH methods. Section 4 presents the discretization process of the Burgers equation using these methods and analyzes the stability of the discrete formulations based on the spectral radius criterion. Section 5 discusses numerical experiments for various forms of the Burgers equations and compares the two methods with other methods in the literature, highlighting the effectiveness and accuracy of KDF-SPH. Finally, Section 6 concludes the paper and offers prospects for future research.

II. The Nonlinear Burgers Equation

The Burgers equation is a simplified form of the Navier-Stokes equations and holds significant importance in fluid dynamics. It describes fluid motion in both compressible and incompressible cases. The formulation of the Burgers equation in the Eulerian coordinate system is as follows:

$$\frac{\partial \boldsymbol{u}_\alpha}{\partial t} + \boldsymbol{u}\cdot\nabla\boldsymbol{u} = \frac{1}{Re}\Delta\boldsymbol{u} \tag{1}$$

The initial value condition of the above equation is

$$\boldsymbol{u}_\alpha(x,0) = \varphi_\alpha(x), \quad x \in \Omega \tag{2}$$

The Dirichlet boundary condition is

$$\boldsymbol{u}_\alpha(x,t) = \zeta_\alpha(x,t), \quad x \in \partial\Omega \tag{3}$$

where $\boldsymbol{u}_\alpha$ is the velocity component in the x_α direction. $\boldsymbol{u}\cdot\nabla\boldsymbol{u}$ represents the nonlinear convection or advection of the velocity field. It describes the transport of momentum due to the fluid's velocity.

The Reynolds number Re is a dimensionless quantity that characterizes the flow regime, representing the ratio of inertial forces to viscous forces in the fluid. The term $\frac{1}{Re}\Delta\boldsymbol{u}$ represents the viscous diffusion of momentum. It describes the effect of viscosity, which tends to smooth out velocity gradients in the fluid.

III. The Meshless Method-SPH Method

In this section, we introduced two types of SPH methods: traditional SPH and the KDF-SPH. These methods will be applied in the subsequent sections to solve the Burgers equation and to analyze their performance.

A. The traditional SPH method

The kernel approximation of a continuous function $f(\boldsymbol{x})$ is expressed as the integral of the product of the kernel function $W(x-\boldsymbol{x}',h)$ and the function $f(\boldsymbol{x})$, represented by the notation $\langle f(\boldsymbol{x})\rangle$ [26].

$$\langle f(\boldsymbol{x})\rangle = \int_\Omega f(\boldsymbol{x}')W(x-\boldsymbol{x}',h)d\boldsymbol{x}' \tag{4}$$

where Ω_W represents the non-negative domain of the kernel function, $W(x-\boldsymbol{x}',h)$ denotes the smoothing kernel function, d indicates the dimensionality of the function, and h is the smoothing length.

The n-th order partial derivative of a continuous function $f(\boldsymbol{x})$, denoted as $\frac{\partial^n f(\boldsymbol{x})}{\partial x_\alpha^n}$, can replace $f(\boldsymbol{x})$ in the aforementioned expression to drive the kernel approximation for $\frac{\partial^n f(\boldsymbol{x})}{\partial x_\alpha^n}$.

$$\left\langle \frac{\partial^n f(\boldsymbol{x})}{\partial x_\alpha^n} \right\rangle = \int_\Omega f(\boldsymbol{x}')\frac{\partial^n}{\partial x_\alpha^n}W(\boldsymbol{x}-\boldsymbol{x}',h)d\boldsymbol{x}' \tag{5}$$

The particle approximation formulation transforms the kernel function expression $W(x-\boldsymbol{x}',h)$ into a discrete form by summing over all particles in the solution domain Ω_W.

$$\langle f(\boldsymbol{x}_i)\rangle \approx \sum_{j=1}^{M} f(\boldsymbol{x}_j)W(\boldsymbol{x}_i-\boldsymbol{x}_j,h)\Delta V_j \tag{6}$$

$$\left\langle \frac{\partial^n f(\boldsymbol{x}_i)}{\partial x_\alpha^n} \right\rangle \approx \sum_{j=1}^{M} f(\boldsymbol{x}_j)\frac{\partial^n}{\partial x_\alpha^n}\left[W(\boldsymbol{x}_i-\boldsymbol{x}_j,h)\right]\Delta V_j \tag{7}$$

where M denotes the total number of particles within the influence domain of the kernel function, and ΔV_j represents the volume of the j-th infinitesimal element dx'. The volume of an infinitesimal element can be expressed in terms of mass

m and density ρ as $\Delta V = \frac{m}{\rho}$.

B. KDF-SPH Method

The Taylor expansion of $f(\boldsymbol{x}')$ at $\boldsymbol{x}$ gives [27]:

$$\begin{aligned} f(\boldsymbol{x}') &= f(\boldsymbol{x}) + \frac{\partial f(\boldsymbol{x})}{\partial x_i}(x_i' - x_i) + \\ &\frac{1}{2}\frac{\partial^2 f(\boldsymbol{x})}{\partial x_i \partial x_j}(x_i' - x_i)(x_j' - x_j) + \dots \\ &= f(\times) + h\frac{\partial f(\boldsymbol{x})}{\partial x_i}\frac{x_i' - x_i}{h} + \\ &\frac{h^2}{2}\frac{\partial^2 f(\boldsymbol{x})}{\partial x_i \partial x_j}\frac{x_i' - x_i}{h}\frac{x_j' - x_j}{h} + \dots \end{aligned} \tag{8}$$

where i and j are summed over their ranges.

By multiplying both sides of (9) by $\frac{x_l' - x_l}{h}W(\boldsymbol{x} - \boldsymbol{x}', h)$, and then integrated over the influence domain of the kernel function. We obtain:

$$\begin{aligned} \left\langle \frac{x_l' - x_l}{h} f(\boldsymbol{x}) \right\rangle &= M_1^l f(\boldsymbol{x}) + hM_2^{il}\frac{\partial f(\boldsymbol{x})}{\partial x_i} \\ &+ \frac{h^2}{2}M_3^{ijk}\frac{\partial^2 f(\boldsymbol{x})}{\partial x_i \partial x_j} + o(h^3) \end{aligned} \tag{9}$$

where

$$M_n^{i^{n_i} j^{n_j} k^{n_k}} = \int_{\Omega_W} \left(\frac{x_i' - x_i}{h}\right)^{n_i} \left(\frac{x_j' - x_j}{h}\right)^{n_j} \left(\frac{x_l' - x_l}{h}\right)^{n_l} \cdot W(x - x', h)dx'$$

are n-moment of the kernel function and $n = n_i + n_j + n_k$. It can be proved that the kernel function's moment constants and independent from h.

Due to the properties of the kernel function moments, it is known that $M_2^{il} = 0$ for $i \neq j$, and $M_3^{ijk} = 0$, we obtain:

$$\frac{\partial f(\boldsymbol{x})}{\partial x_i} = \frac{\left\langle \frac{\boldsymbol{x}_l' - \boldsymbol{x}_l}{h} f(\boldsymbol{x}) \right\rangle - M_1^l f(\boldsymbol{x})}{hM_2^{i^2}} + o(h^2) \tag{10}$$

Similarly, both sides of (9) can be multiplied by $(\frac{x_l' - x_l}{h})^2 W(\boldsymbol{x} - \boldsymbol{x}', h)$, and integrated over the influence domain of the kernel function. We obtain:

$$\begin{aligned} \left\langle \left(\frac{x_l' - x_l}{h}\right)^2 f(\boldsymbol{x}) \right\rangle &= M_2^{l^2} f(\boldsymbol{x}) + hM_3^{ilk}\frac{\partial f(\boldsymbol{x})}{\partial x_i} \\ &+ \frac{h^2}{2}M_4^{ijlk}\frac{\partial^2 f(\boldsymbol{x})}{\partial x_i \partial x_j} + \\ &\frac{h^3}{6}M_5^{ijhlk}\frac{\partial^3 f(\boldsymbol{x})}{\partial x_i \partial x_j \partial x_h} + o(h^4) \end{aligned} \tag{11}$$

Due to the properties of the kernel function moments, it is known that $M_3^{ilk} = 0$ for $i \neq l$, $M_4^{ijlk} = 0$ for $i, j \neq l$, and $M_5^{ijhlk} = 0$. We obtain:

$$\begin{aligned} \frac{\partial^2 f(\boldsymbol{x})}{\partial x_i^2} &= \frac{2}{h^2}\left[M_4^{i^2 l^2}\right]^{-1} \cdot \\ &\left[\left\langle \left(\frac{x_l' - x_l}{h}\right)^2 f(\boldsymbol{x}) \right\rangle - M_2^{l^2} f(\boldsymbol{x})\right] + o(h^2) \end{aligned} \tag{12}$$

IV. Discretized Scheme and Stability Analysis of the Burgers Equation

This section utilizes the one-dimensional Burgers equation as a case study for discretization. Following this, a comprehensive stability analysis is conducted on the resulting discrete formulation to evaluate the validity and robustness of the discretization scheme.

A. Discretized Scheme of the Burgers Equation

In most cases, the SPH requires very small time step, which can significantly slow down the compuatational process. To address this issue and enhance the reliability of the method, a semi-implicit framework is proposed. A one-dimensional model is presented as an example:

$$\begin{aligned} \frac{\partial u(x,t)}{\partial t} + u(x,t)\frac{\partial u(x,t)}{\partial x} &= \frac{1}{Re}\frac{\partial^2 u(x,t)}{\partial x^2} \\ 0 \le x \le L, t > 0, Re > 0 & \end{aligned} \tag{13}$$

The Crank-Nicolson method is initially employed to discretize the aforementioned partial differential equation:

$$\frac{u^{n+1} - u^n}{dt} + \frac{u^n u_x^{n+1} + u^n u_x^n}{2} = \frac{1}{Re}\frac{u_{xx}^{n+1} + u_{xx}^n}{2} \tag{14}$$

By employing the two SPH methods outlined previously and to facilitate the stability analysis of the introduced equation, we represent it in matrix form:

$$\begin{aligned} &\left[I_N + \frac{dt}{2}\left(DK_1 - \frac{1}{Re}K_2\right)\right]U^{n+1} = \\ &\left[I_N - \frac{dt}{2}\left(DK_1 - \frac{1}{Re}K_2\right)\right]U^n \end{aligned} \tag{15}$$

where I_N is an $N \times N$ identity matrix, and matrices K_1 and K_2 represent the approximations of first-order and second-order partial derivatives, respectively, derived through two SPH. The vector D is defined as:

$$D = \begin{pmatrix} u_1^n & \cdots & 0 \\ \vdots & \ddots & \vdots \\ 0 & \cdots & u_N^n \end{pmatrix} \tag{16}$$

B. Stability Analysis of the Burgers Equation

Assuming u in uu_x is a local constant, the error at the n-th time level is defined as follow:

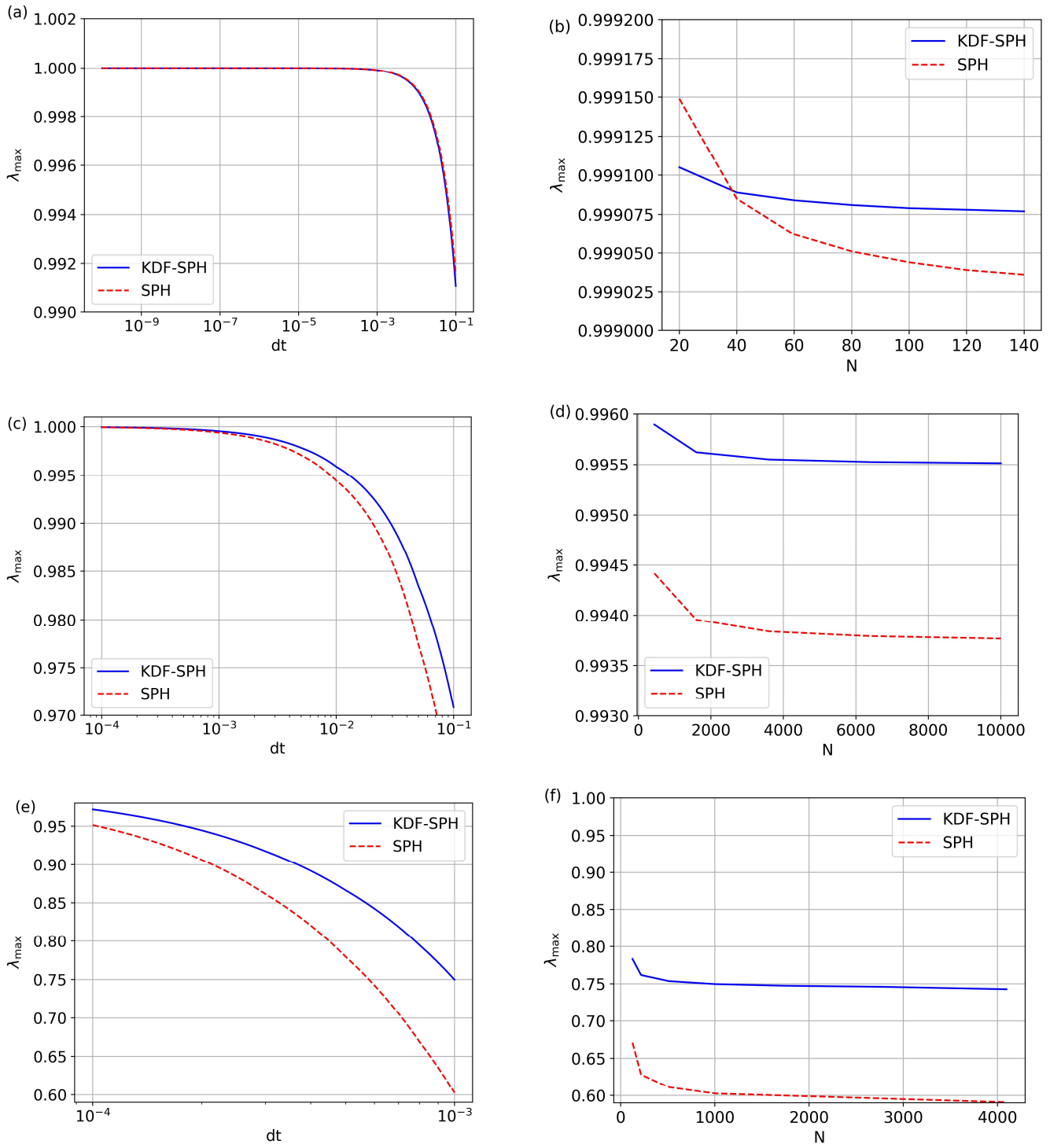

Fig. 2. Spectral radius of 1D, 2D, 3D Burgers equation: (a) 1D Burgers equation of the spectral radius as dt, (b) 1D Burgers equation of the spectral radius as N, (c) 2D Burgers equation of the spectral radius as dt, (d) 2D Burgers equation of the spectral radius as N, (e) 3D Burgers equation of the spectral radius as dt and (f) 3D Burgers equation of the spectral radius as N.

$$e^n = u^n_{\text{exact}} - u^n_{\text{app}} \tag{17}$$

The error equation associated with the discretized Burgers equation, as previously introduced, can be formulated as follows:

$$\left[H + \frac{dt}{2}K\right]e^{n+1} = \left[H - \frac{dt}{2}K\right]e^n \tag{18}$$

where $H = I$, $K = DK_1 - \frac{1}{Re}K_2$. Simplifying, one obtains:

$$e^{n+1} = Pe^n \tag{19}$$

where $P = \left[H + \frac{dt}{2}K\right]^{-1}\left[H - \frac{dt}{2}K\right]$. The numerical scheme's stability is ensured when the 2-norm of the matric P is less than or equal to 1. This condition is equivalent to the spectral radius of the matrix P being less than or equal to

1, denoted as $\rho(P) \le 1$ [28].

Fig. 1 presents the spectral radius plots of the 1D, 2D, and 3D Burgers equations using the SPH and KDF-SPH as dt and N vary. From these six figures, we can clearly observe that, regardless of whether it is the one-dimensional or higher-dimensional Burgers equations, the spectral radius varies with dt and N, remaining less than or equal to one ($\rho(P) \le 1$). This indicates that both methods are stable.

V. Numerical Experiment

In this section, we apply the discretization methods detailed in the previous section to benchmark our results against those derived from other numerical methods. We perform numerical computations and simulations for various Burgers equation, including those defined on irregular domains. All numerical experiments in this section utilize cubic B-spline kernel functions [29], [30]. To validate the effectiveness of the proposed methods, we conduct an error analysis based on the infinity norm (denoted by the infinity symbol), which is defined as follows:

$$L_\infty = \max_{1 \le j \le N} |U_j - u_j| \tag{20}$$

where u_j represents exact solution of $u(x,t)$ and U_j is the numerical solution.

The kernel function $W(x-x',h)$ is defined as:

$$W(x-x',h) = \frac{\alpha_d}{h^d} \begin{cases} \frac{2}{3} - s^2 + \frac{1}{2}s^3 & 0 \le s < 1 \\ \frac{1}{6}(2-s)^3 & 1 \le s < 2 \\ 0 & s \ge 2 \end{cases} \tag{21}$$

where d represents the dimension of the function, and s is defined as $s = \frac{r}{h}$. Where $r = |x - x'|$ is the distance between points x' and x. Additionally, α_d takes the values of 1, $\frac{15}{7\pi}$ and $\frac{3}{2\pi}$ for 1D, 2D, and 3D cases respectively.

Example 1. We consider the following 1D Burgers equation [31], [32]:

$$\frac{\partial u(x,t)}{\partial t} + u(x,t)\frac{\partial u(x,t)}{\partial x} = \frac{1}{Re}\frac{\partial^2 u(x,t)}{\partial x^2} \tag{22}$$

where the ranges of x and t are $0 \le x \le 2$, $0 < t \le T$. With the initial condition is:

$$u(x,0) = 2\pi \frac{1}{Re} \frac{\sin(\pi x) + 4\sin(2\pi x)}{4 + \cos(\pi x) + 2\cos(2\pi x)}, 0 < x < 2 \tag{23}$$

and the Dirichlet boundary value condition is:

$$u(0,t) = 0, \quad u(2,t) = 0, \quad 0 < t \le T \tag{24}$$

Let $G = \exp\left(-\pi^2 \frac{1}{Re} t\right)$ and $L = \exp\left(-4\pi^2 \frac{1}{Re} \frac{2}{t}\right)$. Then, the analytical solution is:

$$u(x,t) = 2\pi \frac{1}{Re} \frac{\sin(\pi x)G + 4\sin(2\pi x)L}{4 + \cos(\pi x)G + 2\cos(2\pi x)L} \tag{25}$$

TABLE I
Comparison of The L_∞ Error for Example 1 at Time $T = 0.1$ s

Method	$\Delta x = 1/20$	$\Delta x = 1/40$	$\Delta x = 1/80$
SPH	1.499×10^{-1}	6.513×10^{-2}	3.050×10^{-2}
KDF-SPH	4.352×10^{-2}	1.674×10^{-2}	6.647×10^{-3}

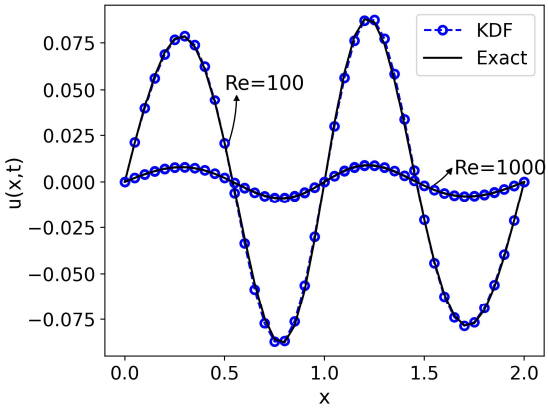

Fig. 2. Simulation results of Example 1 at various Re

Table I compares the L_∞ error of the $|u|$ generated by both SPH and KDF-SPH in solving the 1D Burgers equation at different spatial steps ($\Delta x = 1/20, 1/40, 1/80$) with $Re = 1$. The results indicate that KDF-SPH produces significantly smaller errors than SPH at the same spatial step sizes. Furthermore, these findings confirm the effectiveness of the proposed approach in solving the 1D Burgers equation, as it significantly reduces errors and improves convergence accuracy.

To further illustrate the accuracy of the method, Table II presents a comparison of the L_∞ errors between the KDF-SPH and other methods at two different time instances, $T = 0.1$ s and $T = 1$ s, for various Re values. The results demonstrate that KDF-SPH achieves better accuracy in terms of error rates, indicating its superior performance in simulating the one-dimensional Burgers equation.

Fig. 2 compares numerical results from KDF-SPH with the analytical solution for $Re = 100$ and $Re = 1000$. The comparison is conducted under conditions: $\Delta t = 1/100$, $\Delta x = 1/20$, and $T = 0.1$ s. The solid black line represents the analytical solution, whereas the blue line denotes the numerical solution obtained from KDF-SPH. The figure clearly shows that the numerical results align well with the analytical solution across different Re values, simplifying the accuracy and reliability of the proposed method.

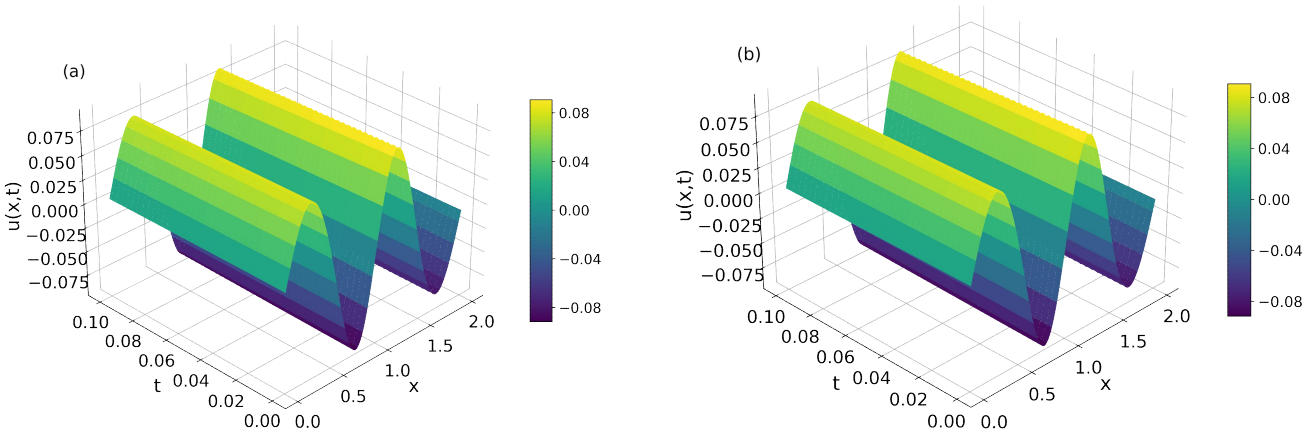

Fig. 3. Comparison of numerical and exact solution through KDF-SPH for Example2

TABLE II

COMPARATIVE STUDY OF THE L_∞ ERROR BETWEEN DIFFERENT METHODS FOR EXAMPLE 1

Re	$T=0.1$ s			$T=1$ s		
	[31]	[32]	KDF-SPH	[31]	[32]	KDF-SPH
10^2	4.41×10^{-3}	3.13×10^{-3}	3.37×10^{-3}	3.13×10^{-2}	2.12×10^{-2}	1.44×10^{-2}
10^3	4.60×10^{-5}	4.30×10^{-5}	3.68×10^{-5}	4.45×10^{-4}	4.15×10^{-4}	3.38×10^{-4}
10^4	4.62×10^{-7}	4.42×10^{-7}	3.68×10^{-7}	4.61×10^{-6}	4.40×10^{-6}	3.65×10^{-6}
10^5	4.62×10^{-9}	4.46×10^{-9}	3.70×10^{-9}	4.62×10^{-8}	4.43×10^{-8}	3.68×10^{-8}

TABLE III

COMPARISON OF THE L_∞ ERROR FOR EXAMPLE 2 AT $T=0.5$ S

Method	$(\Delta x,\Delta y)=(\frac{1}{20},\frac{1}{20})$	$(\Delta x,\Delta y)=(\frac{1}{40},\frac{1}{40})$	$(\Delta x,\Delta y)=(\frac{1}{60},\frac{1}{60})$	$(\Delta x,\Delta y)=(\frac{1}{80},\frac{1}{80})$
SPH	9.328×10^{-5}	4.741×10^{-5}	3.173×10^{-5}	2.384×10^{-5}
KDF-SPH	1.125×10^{-5}	5.679×10^{-6}	3.800×10^{-6}	2.960×10^{-6}

TABLE IV

COMPARATIVE STUDY OF THE L_∞ ERROR BETWEEN DIFFERENT METHODS FOR EXAMPLE 2

$(\Delta x,\Delta y)$	$Re=1$		$Re=10$	
	[33]	KDF-SPH	[33]	KDF-SPH
$(\frac{1}{20},\frac{1}{20})$	1.4830×10^{-4}	1.1755×10^{-4}	3.0770×10^{-3}	1.9928×10^{-3}
$(\frac{1}{40},\frac{1}{40})$	2.9210×10^{-4}	5.9315×10^{-5}	1.6260×10^{-2}	7.5417×10^{-4}
$(\frac{1}{80},\frac{1}{80})$	5.8200×10^{-4}	2.9750×10^{-5}	3.8200×10^{-2}	3.2259×10^{-4}

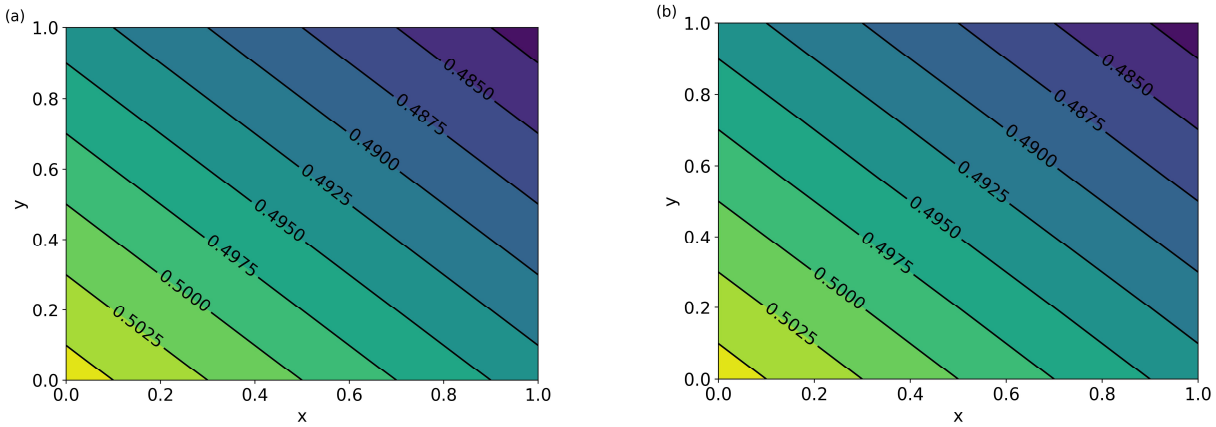

Fig. 4. Simulation results of Example 2 through KDF-SPH at $T=0.5$ s: (a) Numerical solution of u , (b) Analytic solution of u .

Fig. 3 presents a comparison of the numerical solution and the analytical solution for $Re = 100$, $\Delta t = 0.001$, $\Delta x = 1/20$, and $T = 0.1$ s. In this figure, (a) represents the numerical solution obtained using the KDF-SPH, while (b) represents the exact solution. The image demonstrates a minimal error between the numerical and exact solutions, confirming the reliability of the numerical method.

Example 2. We consider the following 2D Burgers equation with Dirichlet boundary conditions:

$$\frac{\partial u}{\partial t} + u\frac{\partial u}{\partial x} + v\frac{\partial u}{\partial y} = \frac{1}{Re}\left(\frac{\partial^2 u}{\partial x^2} + \frac{\partial^2 u}{\partial y^2}\right) \quad (x, y) \in \Omega, t > 0 \quad (26)$$

with the analytical solution is

$$u(x, y, t) = \frac{1}{1 + e^{\frac{Re(x+y-t)}{2}}} \quad (27)$$

and the Dirichlet boundary condition can be obtained by the above analytical solution.

Table III compares the L_∞ -norm errors between SPH and KDF-SPH across various spatial steps for Re =0.1. The results indicate that KDF-SPH consistently outperforms SPH. This demonstrates its effectiveness in simulating the Burgers equation. To further validate the method, we compare the L_∞ error under different $(\Delta x, \Delta y)$ resolutions at $Re = 1$ and $Re = 10$, with $T = 0.25$ s, against the results from [33] in Table IV. The findings confirm that KDF-SPH provides superior accuracy and effectiveness.

To illustrate the accuracy of the proposed method in Example 2, Fig. 4 compares numerical and analytical solutions of u for $Re = 0.1$ and $T = 0.5$ s. Using a spatial step size of $(1/40, 1/40)$, the results from KDF-SPH show strong agreement with the analytical solution.

Fig. 5 presents numerical solutions for four irregular domains: a trilobed region, a star-shaped region, a pentagram-shaped region, and a gear-shaped region, with a spatial step size of $(1/40, 1/40)$. The fitting effect is very good, showing the accuracy of the numerical solutions. Additionally, Table V shows that KDF-SPH exhibits significantly higher precision when simulating these four types of regions. These results demonstrate the robustness of the proposed method in solving the 2D Burgers equation in irregular domains.

TABLE V
NUMERICAL SOLUTION ERROR IN FOUR IRREGULAR DOMAINS FOR EXAMPLE 2

Irregular Domains	L_∞ (SPH)	L_∞ (KDF-SPH)
Trilobed Region	1.892×10^{-3}	5.401×10^{-4}
Star-shaped Region	2.105×10^{-3}	4.961×10^{-4}
Pentagram-shaped Region	1.584×10^{-3}	2.903×10^{-3}
Gear-shaped Region	3.573×10^{-3}	2.126×10^{-4}

Example 3. In fluid dynamics, the two-dimensional coupled Burgers equations represent a set of particle differential equations that govern the behavior of velocity fields. These equations are widely utilized in fluid dynamics, turbulence

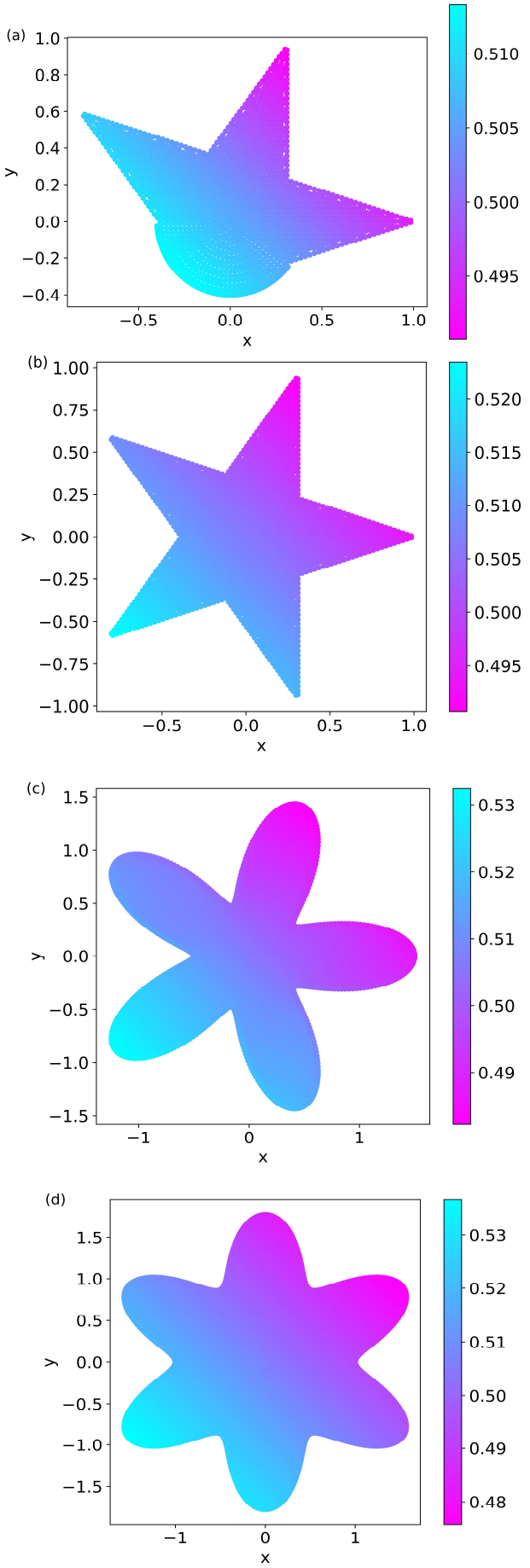

Fig. 5. Numerical simulation of the solution u in four irregular domain for Example 2: (a) A trilobed region, (b) A star-shaped region, (c) A pentagram-shaped region, (d) A gear-shaped region.

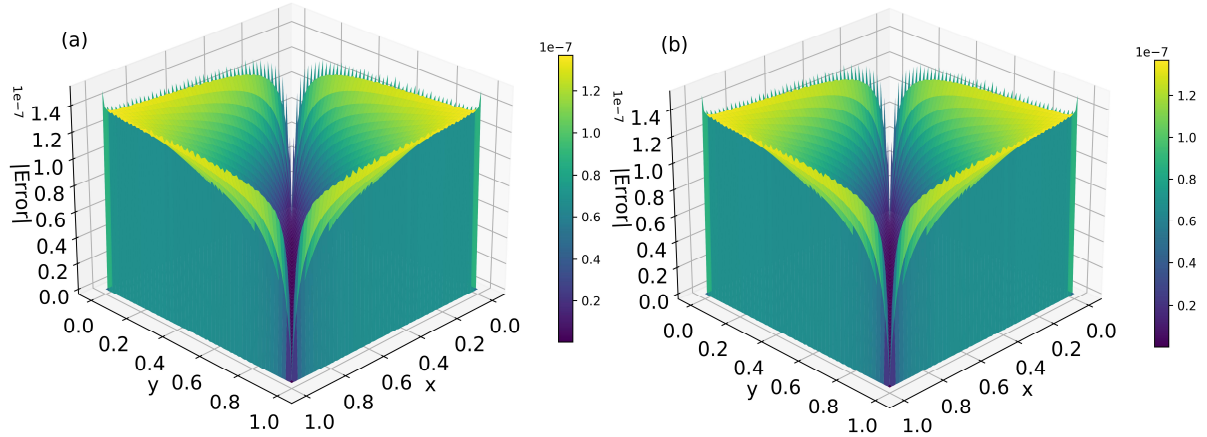

Fig. 6. Overall error through KDF-SPH for Example 3: (a) A trilobed region, (b) A star-shaped region, (c) A pentagram-shaped region, (d) A gear-shaped region.

TABLE VI
COMPARISON OF THE L_∞ ERROR FOR EXAMPLE 3 AT TIME $T = 0.5$ S

$(\Delta x, \Delta y)$	SPH		KDF-SPH	
	$u(x,y,t)$	$v(x,y,t)$	$u(x,y,t)$	$v(x,y,t)$
$(1/20, 1/20)$	6.40×10^{-6}	6.40×10^{-6}	6.92×10^{-7}	6.92×10^{-7}
$(1/40, 1/40)$	2.99×10^{-6}	2.99×10^{-6}	3.60×10^{-7}	3.60×10^{-7}
$(1/60, 1/60)$	2.01×10^{-6}	2.01×10^{-6}	2.40×10^{-7}	2.40×10^{-7}
$(1/80, 1/80)$	1.51×10^{-6}	1.51×10^{-6}	1.81×10^{-7}	1.81×10^{-7}

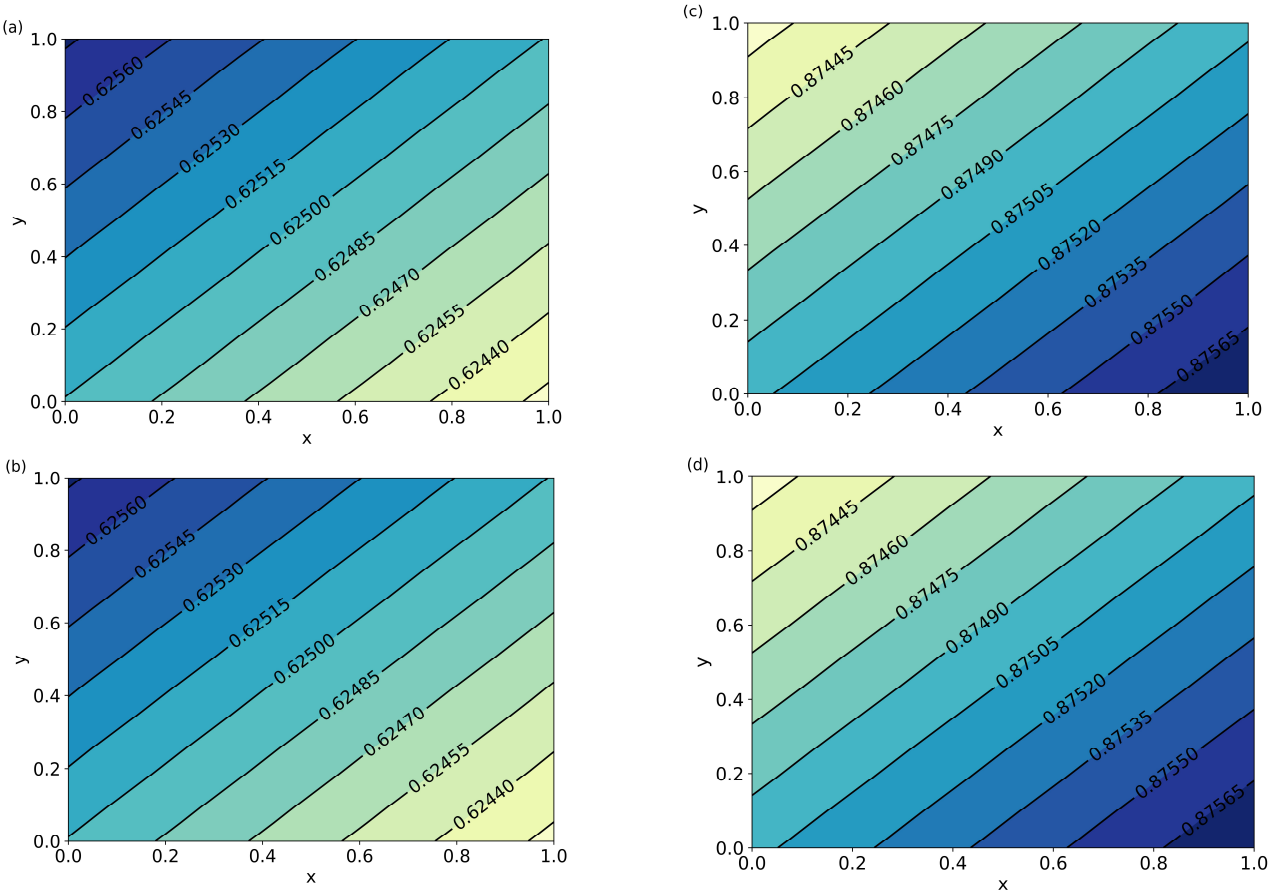

Fig. 7. Simulation results through KDF-SPH for Example 3: (a) Numerical solution of u, (b) Analytic solution of u, (c) Numerical solution of v, (d) Analytic solution of v.

modeling, and the study of nonlinear wave phenomena, making them significant in both physics and engineering applications [34]. Therefore, we consider the following 2D coupled Burgers equation:

$$\begin{cases} \dfrac{\partial u}{\partial t}+u\dfrac{\partial u}{\partial x}+v\dfrac{\partial u}{\partial y}=\dfrac{1}{Re}\left(\dfrac{\partial^2 u}{\partial x^2}+\dfrac{\partial^2 u}{\partial y^2}\right) \\ \dfrac{\partial v}{\partial t}+u\dfrac{\partial v}{\partial x}+v\dfrac{\partial v}{\partial y}=\dfrac{1}{Re}\left(\dfrac{\partial^2 v}{\partial x^2}+\dfrac{\partial^2 v}{\partial y^2}\right) \end{cases} \tag{28}$$

with the analytical solution is:

$$\begin{cases} u(x,y,t)=\dfrac{3}{4}-\dfrac{1}{4\left[1+e^{\frac{\mathrm{Re}(-4x+4y-t)}{32}}\right]} \\ v(x,y,t)=\dfrac{3}{4}+\dfrac{1}{4\left[1+e^{\frac{\mathrm{Re}(-4x+4y-t)}{32}}\right]} \end{cases} \tag{29}$$

and the Dirichlet boundary condition can be obtained by the above analytical solution.

Fig. 6 presents a comparative analysis of the overall errors for the velocity components u and v at $T=0.5$ s and $Re=0.1$. The symmetric distribution of errors indicates strong agreement between the KDF-SPH results and the analytical solutions. Furthermore, Fig. 7 simulates the solution of the 2D coupled Burgers equation using two SPH methods. For $Re=0.1$, $(\Delta x,\Delta y)=(1/20,1/20)$ and $T=0.5$ s, the numerical and analytical solutions for u and v are compared. The results show good agreement, with errors smaller than those from SPH. This demonstrates that KDF-SPH effectively models the coupled 2D Burgers equation system.

Table VI compares the errors in u and v for two different SPH methods at $Re=0.1$ and $T=0.5$ s, with different spatial steps. The results indicate that KDF-SPH outperforms SPH across four different particle counts, with errors decreasing as the number of particles increases. This Burgers equation is given by:

$$\frac{\partial u}{\partial t}+u\left(\frac{\partial u}{\partial x}+\frac{\partial u}{\partial y}+\frac{\partial u}{\partial z}\right)=\frac{1}{Re}\left(\frac{\partial^2 u}{\partial x^2}+\frac{\partial^2 u}{\partial y^2}+\frac{\partial^2 u}{\partial z^2}\right) \tag{30}$$

with the analytical solution is:

$$u(x,y,z,t)=\frac{2\cdot a\cdot\pi\cdot e^{-\frac{3\cdot a^2}{Re}\pi^2\cdot t}\cdot\sin(a\cdot\pi\cdot(x+y+z))}{Re\cdot\left(\alpha+e^{-\frac{3\cdot a^2}{Re}\cdot\pi^2\cdot t}\cdot\cos(a\cdot\pi\cdot(x+y+z))\right)} \tag{31}$$

and the Dirichlet boundary condition can be obtained by the above analytical solution.

Fig. 8 illustrates a comparison between the numerical solution obtained using KDF-SPH and the analytical solution for the 3D Burgers equation with $Re=10$, $\alpha=5$ and spatial step $(\Delta x,\Delta y,\Delta z)=(1/10,1/10,1/10)$. The comparison shows that KDF-SPH achieves excellent agreement with the analytical solution, confirming the accuracy of the proposed method. Additionally, Table VII presents a comparison of the errors between the two methods at different spatial step sizes. The analysis reveals that KDF-SPH exhibits superior accuracy over traditional SPH, with errors decreasing as the number of particles increases. This reduction in error further demonstrates the efficacy of KDF-SPH in resolving the three-dimensional Burgers equation. The improved performance of KDF-SPH can be attributed to its enhanced kernel approximation, which effectively handles the complexities of higher-dimensional problems. Furthermore, the method's ability to maintain stability and accuracy across a wide range of Reynolds numbers and spatial resolutions underscores its robustness.

Example 5. Next, we proceed to consider the three-dimensional coupled Burgers equations and simulate them using two methods to compare their errors. The equations are as follows:

$$\begin{cases} \dfrac{\partial u}{\partial t}+u\dfrac{\partial u}{\partial x}+v\dfrac{\partial u}{\partial y}+w\dfrac{\partial u}{\partial z}=\dfrac{1}{Re}\left(\dfrac{\partial^2 u}{\partial x^2}+\dfrac{\partial^2 u}{\partial y^2}+\dfrac{\partial^2 u}{\partial z^2}\right) \\ \dfrac{\partial v}{\partial t}+u\dfrac{\partial v}{\partial x}+v\dfrac{\partial v}{\partial y}+w\dfrac{\partial v}{\partial z}=\dfrac{1}{Re}\left(\dfrac{\partial^2 v}{\partial x^2}+\dfrac{\partial^2 v}{\partial y^2}+\dfrac{\partial^2 v}{\partial z^2}\right) \\ \dfrac{\partial w}{\partial t}+u\dfrac{\partial w}{\partial x}+v\dfrac{\partial w}{\partial y}+w\dfrac{\partial w}{\partial z}=\dfrac{1}{Re}\left(\dfrac{\partial^2 w}{\partial x^2}+\dfrac{\partial^2 w}{\partial y^2}+\dfrac{\partial^2 w}{\partial z^2}\right) \end{cases} \tag{32}$$

Let $Q=e^{\frac{a^2+b^2+c^2}{Re}\pi^2\cdot t}$, $\omega=a\cdot\pi\cdot x$, $\psi=b\cdot\pi\cdot y$, $\zeta=c\cdot\pi\cdot z$, then the analytical solution is:

$$\begin{cases} u(x,y,z,t)=-\dfrac{2\cdot a\cdot\pi\cdot Q\cdot\cos\omega\cdot\sin\psi\cdot\sin\zeta}{Re\left(\alpha+Q\cdot\sin\omega\cdot\sin\psi\cdot\sin\zeta\right)} \\ v(x,y,z,t)=-\dfrac{2\cdot b\cdot\pi\cdot Q\cdot\sin\omega\cdot\cos\psi\cdot\sin\zeta}{Re\left(\alpha+Q\cdot\sin\psi\cdot\sin\zeta\right)} \\ w(x,y,z,t)=-\dfrac{2\cdot c\cdot\pi\cdot Q\cdot\sin\omega\cdot\sin\psi\cdot\cos\zeta}{Re\left(\alpha+Q\cdot\sin\omega\cdot\sin\psi\cdot\sin\zeta\right)} \end{cases} \tag{33}$$

and the Dirichlet boundary condition can be obtained by the above analytical solution.

Table VIII presents the numerical simulation results for the coupled three-dimensional Burgers equation using two different methods under the parameters $Re=100$, $T=0.1$ s, $a=1$, $b=1$, and $c=1$. The table provides a comparative analysis of the associated errors for different spatial steps. The results show that both methods are applicable to the equation set; however, KDF-SPH exhibits significantly reduced numerical solutions for all three velocity components compared to SPH. Furthermore, KDF-SPH demonstrates a consistent decrease in error as the number of number of particles increases. It is more accurate for solving the three-dimensional Burgers equations and is a better tool for numerical simulations.

VI. Conclusion

In this paper, we present a numerical approach based on SPH and KDF-SPH method, combined with the finite various

TABLE VII
COMPARISON OF THE L_∞ ERROR FOR EXAMPLE 4 AT $T = 0.1$ S AND $\alpha = 0.5$

Method	$(\Delta x, \Delta y, \Delta z) = (\frac{1}{10}, \frac{1}{10}, \frac{1}{10})$	$(\Delta x, \Delta y, \Delta z) = (\frac{1}{15}, \frac{1}{15}, \frac{1}{15})$	$(\Delta x, \Delta y, \Delta z) = (\frac{1}{20}, \frac{1}{20}, \frac{1}{20})$
SPH	1.085×10^{-4}	6.349×10^{-5}	4.870×10^{-5}
KDF-SPH	3.719×10^{-5}	3.557×10^{-5}	3.557×10^{-5}

TABLE VIII
COMPARISON OF THE L_∞ ERROR FOR EXAMPLE 5 AT TIME $T = 0.1$ S AND $\alpha = 0.5$

$(\Delta x, \Delta y, \Delta z)$	SPH			KDF-SPH		
	$u(x,y,z,t)$	$v(x,y,z,t)$	$w(x,y,z,t)$	$u(x,y,z,t)$	$v(x,y,z,t)$	$w(x,y,z,t)$
$(\frac{1}{10}, \frac{1}{10}, \frac{1}{10})$	1.873×10^{-3}	1.873×10^{-3}	7.890×10^{-3}	8.768×10^{-5}	1.061×10^{-4}	5.027×10^{-3}
$(\frac{1}{15}, \frac{1}{15}, \frac{1}{15})$	1.955×10^{-3}	1.965×10^{-3}	9.250×10^{-3}	4.721×10^{-5}	7.492×10^{-5}	6.898×10^{-3}
$(\frac{1}{20}, \frac{1}{20}, \frac{1}{20})$	1.982×10^{-3}	1.986×10^{-3}	9.991×10^{-3}	3.907×10^{-5}	6.810×10^{-5}	8.178×10^{-3}

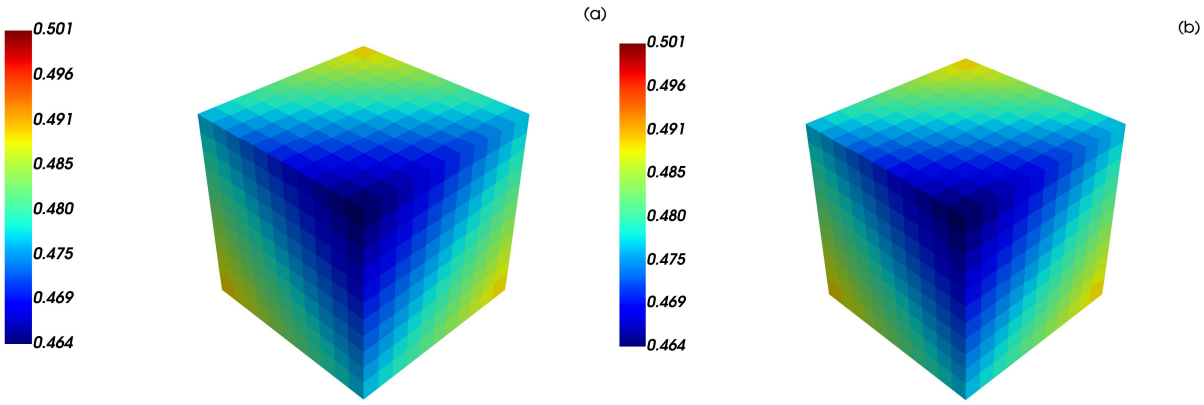

Fig. 8. Simulation results through KDF-SPH for Example 4: (a) Numerical solution of u, (b) Analytic solution of u.

method for solving the Burgers equation. Due to the nonlinear nature of the Burgers equation, implicit schemes often lead to high computational costs. To address this issue, we propose a semi-implicit scheme, whose unconditional stability is demonstrated through a stability analysis. The effectiveness and accuracy of the proposed scheme are quantified by comparing numerical solutions with exact solutions in 1D, 2D, and 3D test cases. The results show that KDF-SPH outperforms traditional SPH and other methods in the literature, making it more suitable for solving the Burgers equation.

In future work, we aim to develop more efficient methods for handling nonlinear terms to further reduce computational time and enhance accuracy. Additionally, we plan to extend the proposed approach to solve other type of Burgers equation, such as fractional Burgers equation or coupled Burgers systems, to explore its applicability in a wider range of fluid dynamics problems.

REFERENCES

[1] S. Q. Ding, "Qualitative properties of solutions for a class of bistable type Burgers equation," M.S. thesis, Nanjing University of Finance and Economics, Nanjing, China, DOI: 10.27705/d.cnki.gnjcj.2023.000391.

[2] S. Elbostani, and R. El Jid, "A Meshless Method Based on the Moving Least Squares Approach for Approximate Solution of the Generalized 2-D Nonlinear Benjamin-Bona-Mahony-Burgers Equation," *IAENG International Journal of Applied Mathematics*, vol. 54, no. 9, pp1734-1746, 2024.

[3] J. M. Burgers, "A mathematical model illustrating the theory of turbulence," *Advances in Applied Mechanics*, Vol. 1, pp. 171-199, 1948.

[4] X. Zhang and B. Zhuang, "Cubic B-spline collocation method for the numerical solution of time fractional order Burgers equations," Numerical Mathematics: A Journal of Chinese Universities, Vol. 44, No. 4, pp. 311-328, 2022.

[5] L. Chen, "Several finite difference methods for one-dimensional Burgers equation," M.S. thesis, China West Normal University, Nanchong, China, 2019.

[6] X. Wang, Q. Zhang, and Z. Sun, "The pointwise error estimates of two energy-preserving fourth-order compact schemes for viscous Burgers' equation," *Advances in Computational Mathematics*, Vol. 47, No. 2, 2021.

[7] Q. Zhang, Y. Qin, and Z. Sun, "Linearly compact scheme for 2D Sobolev equation with Burgers' type nonlinearity," *Numerical Algorithms*, Vol. 91, No. 3, pp. 1081-1114, 2022.

[8] C. Xu and L. Pei, "Unconditional superconvergence analysis of two modified finite element fully discrete schemes for nonlinear Burgers' equation," *Applied Numerical Mathematics*, Vol. 185, pp. 1-17, 2023.

[9] C. Wang and T. W. Jun, "A multi-domain Galerkin method with numerical integration for the Burgers equation," *International Journal of Computer Mathematics*, Vol. 100, No. 5, pp. 927-947, 2023.

[10] Z. Zhao and H. Li, "Numerical study of two-dimensional Burgers' equation by using a continuous Galerkin method," *Computers and Mathematics with Applications*, Vol. 149, pp. 38-48, 2023.

[11] H. Wang, D. Xu, J. Zhou, and J. Guo, "Weak Galerkin finite element method for a class of time fractional generalized Burgers' equation," *Numerical Methods for Partial Differential Equations*, Vol. 37, No. 1, pp. 732-749, 2020.
[12] G. H. Sun, Z. Wang, J. Nie, et al., "Generalized finite difference method for a class of multidimensional space-fractional diffusion equations," *Computational Mechanics*, Vol. 67, No. 1, pp. 1-16, 2020.
[13] L. Wang, F. Xu, and Y. Yang, "Improvement of the tensile instability in SPH scheme for the FEI (Fluid-Elastomer Interaction) problem," *Engineering Analysis with Boundary Elements*, Vol. 106, pp. 116-125, 2019.
[14] P. N. Sun, S. Marrone, A. Colagrossi, and A. M. Zhang, "The delta plus-SPH model: Simple procedures for a further improvement of the SPH scheme," *Computer Methods in Applied Mechanics and Engineering*, Vol. 315, pp. 25-49, Mar. 2017.
[15] C. Huang, et al., "A kernel gradient-free SPH method with iterative particle shifting technology for modeling low-Reynolds flows around airfoils," *Engineering Analysis with Boundary Elements*, Vol. 106, pp. 571-587, 2019.
[16] J. Ren, et al., "An improved parallel SPH approach to solve 3D transient generalized Newtonian free surface flows," *Computer Physics Communications*, Vol. 205, pp. 87-105, 2016.
[17] X. F. Yang, S. L. Peng, and M. B. Liu, "A new kernel function for SPH with applications to free surface flows," *Applied Mathematical Modelling*, Vol. 38, No. 15-16, pp. 3822-3833, 2014.
[18] L. B. Lucy, "A numerical approach to the testing of the fission hypothesis," *Astronomical Journal*, Vol. 82, pp. 1013-1024, 1977.
[19] R. A. Gingold and J. J. Monaghan, "Smoothed particle hydrodynamics: theory and application to non-spherical stars," *Monthly Notices of the Royal Astronomical Society*, Vol. 181, pp. 375-389, 1977.
[20] M. B. Liu and G. R. Liu, "Smoothed Particle Hydrodynamics (SPH): an Overview and Recent Developments," *Archives of Computational Methods in Engineering*, Vol. 17, No. 1, pp. 1-52, 2009.
[21] J. J. Monaghan, "Smoothed Particle Hydrodynamics and Its Diverse Applications," *Annual Review of Fluid Mechanics*, Vol. 44, No. 1, pp. 323-346, 2012.
[22] J. J. Monaghan, "Simulating free surface flows with SPH," *Journal of Computational Physics*, Vol. 110, pp. 399-406, 1994.
[23] S. Li and W. K. Liu, "Meshfree and particle methods and their applications," *Applied Mechanics Reviews*, Vol. 55, No. 1, pp. 1-34, 2002.
[24] Z. L. Zhang and M. B. Liu, "Numerical studies on explosive welding with ANFO by using a density adaptive SPH method," *Journal of Manufacturing Processes*, Vol. 41, pp. 208-220, 2019.
[25] D. Violeau and B. D. Rogers, "Smoothed particle hydrodynamics (SPH) for free-surface flows: past, present and future," *Journal of Hydraulic Research*, Vol. 54, No. 1, pp. 1-26, 2016.
[26] J. J. Monaghan and A. Kocharyan, "SPH simulation of multi-phase flow," *Computer Physics Communications*, Vol. 87, pp. 225-235, 1995.
[27] D. Feng and R. Imin, "A kernel derivative free SPH method," *Results in Applied Mathematics*, Vol. 17, 2023
[28] Siraj-ul-Islam, A. A. Ali, S. Haq, "A computational modeling of the behavior of the two-dimensional reaction diffusion Brusselator system," *Applied Mathematical Modelling*, Vol. 34, No. 12, pp. 3896-3909, 2010.
[29] M. B. Liu and G. R. Liu, "Meshfree particle simulation of micro channel flows with surface tension," *Computational Mechanics*, Vol. 35, No. 5, pp. 332-341, 2005.
[30] J. J. Monaghan and H. Pongracic, "Artificial viscosity for particle methods," *Applied Numerical Mathematics*, Vol. 1, No. 3, pp. 187-194, 1985.
[31] G. Arora and B. K. Singh, "Numerical solution of Burgers' equation with modified cubic B-spline differential quadrature method," *Applied Mathematics and Computation*, Vol. 224, pp. 166-177, 2013.
[32] L. Li, "Sinc collocation method for solving several classes of differential equations," M.S. thesis, Jiangsu University, Zhenjiang, China. DOI:10.27170/d.cnki.gjsuu.2021.001034.
[33] Y. Duan and R. Liu, "Lattice Boltzmann model for two-dimensional unsteady Burgers' equation," *Journal of Computational and Applied Mathematics*, Vol. 206, No. 1, pp. 432-439, 2006.
[34] A. Sreelakshmi, V. P. Shyaman, and A. Awasthi, "An integrated stairwise adaptive finite point scheme for the two-dimensional coupled Burgers' equation," *Fluid Dynamics Research*, Vol. 56, No. 6, 2024.